

Analysis of the wind speed as a function of the height of the atmospheric boundary layer

A. Benaboud¹, A. Echchelh^{1,*}, A. Saad¹, M. Hajjoubi², Karrouk. M. S. ², F. Lahlou¹

¹Laboratory of Electrical Engineering and Energetic Systems, IbnTofail University, Kenitra, Morocco

²Laboratoire de Climatologie et télédétection, Université Hassan II, FLSH Ben M'Sick

Email address

echeladil@yahoo.fr (A. Echchelh)

To cite this article

A. Benaboud, A. Echchelh, A. Saad, M. Hajjoubi, Karrouk. M. S., F. Lahlou. Analysis of the Wind Speed as a Function of the Height of the Atmospheric Boundary Layer, *American Journal of Energy Science*. Vol. 1, No. 1, 2014, pp. 1-6

Abstract

The aim of this work is to model the wind speed profile in a semi-arid area based on the thermal stability of the atmosphere. The velocity profiles are measured under optimal conditions by the Centre for Development of Renewable Energy CDER. The data is collected every 10 minutes at heights ranging from 10 to 50 m above the ground using a tower installed on the Wind Park Koudia Al Baida (the region of Tanger Tetouan). The atmospheric stability classes, thus defined, the vertical profiles of tracks wind speed show that when the atmospheric conditions are unstable, the air movement is strongly turbulent and profile tends towards uniformity. By cons, if the conditions are stable profile is close enough to where the data is processed globally irrespective stability classes.

Keywords

Atmospheric Stability, Vertical Wind Profile, Roughness, Similarity Theory

1. Introduction

The wind is defined as the direction from which it comes (Tw); and not by the direction it goes, which is logical because it is the source of wind that defines his character: In Morocco the north wind is cold, the south wind is warm, the east wind is dry, the west wind is wet ... while the destination of the wind provides no information about its nature. The wind direction is expressed in aviation using the compass of directions 36. His arrow is in the direction of travel. On aerodromes of low importance, the wind direction is referenced using sleeved tees air or landing. While in Aerodromes of great importance, the vane is connected to a recorder assumption of similarity Monin-Obukov is currently the most commonly used to describe the vertical variation of the wind speed as a function of altitude in the low atmospheric boundary layer. This theory has been completed by the work of Dryer 1974 and Paulson 1970, who gave the expressions of implicit functions for different roughness classes, the purpose of this study is to model the wind profile in a semi -arid area based thermal

stability of the atmosphere. The wind (speed and direction) and lighting (solar and reflected) necessary data is provided by CDER

(Center for Renewable Energy Development). These data are measured at levels ranging from 10 to 50 m of soil data using a pylon installed on the Wind Park Koudia Al Baida (the region Tanger Tetouan). After treatment (empty and coherence) data were established according to the stability classes as a function of to the length of Monin - Obukov, which allowed the plot of the vertical wind profile, depending on weather conditions encountered.

2. Materials and Methods

The Obukov the length (L) is a parameter having a length dimension used in micro meteorology, in meteorological convection and atmospheric dispersion. It describes the effects of buoyancy (vector sum of the buoyancy and weight of the air) on the turbulent flow, mainly in the lower portion of the atmospheric boundary layer. It was introduced for the first time in 1946 by Alexander Obukov. It is also known as Monin Obukov

length, given its importance in the similarity theory developed by Monin and Obukov.

Obukhov length depends on the turbulence and sensible heat flux H by:

$$L = -\frac{u_*^3 \overline{\theta_v}}{kg \left(\frac{H}{\rho c_p}\right)} \quad (1)$$

Where u_* the friction velocity, $\overline{\theta_v}$ the average potential virtual temperature, ρ the density of the air, c_p its specific heat capacity, g the acceleration of gravity and k is the von Karman constant [13]. The stability parameter, ζ is defined as z/L , where z is commonly used measurement height:

$$\zeta = \frac{z}{L} = -\frac{kgz \left(\frac{H}{\rho c_p}\right)}{u_*^3 \overline{\theta_v}} \quad (2)$$

Applied for a flat and homogeneous field, the Monin-Obukov theory is based on the assumption that the average gradient of the wind speed depends on a variable universal function variable under the conditions of stability of the atmospheric boundary layer [16]. Conditions that may be neutral (turbulence forces are in equilibrium), stable or unstable (according to the predominance of the forces acting on air masses). The Monin-Obukov expression [1], giving the velocity profile wind is written as:

$$V(z) = \frac{u_*}{k} \left[\ln\left(\frac{z}{z_0}\right) - \Psi_M\left(\frac{z}{L}\right) + \Psi_M\left(\frac{z_0}{L}\right) \right] \quad (3)$$

U_* : Speed of friction, ms⁻¹.

Z : Altitude of the site, m.

Z_0 : Roughness of soil, m.

L : Length Monin-Obukov, m.

Ψ_M : Implicit functions.

The expression of the universal function Ψ_M depend of atmospheric stability class defined by the Monin-Obukov length

[2, 3] as:

$$\Psi_M = 2 \ln\left(\frac{1+x}{2}\right) + \ln\left(\frac{1+x^2}{2}\right) - 2 \operatorname{Arctan}(x) + \frac{\pi}{2}$$

$$\text{For } L < 0 \quad (\text{if unstable}) \quad (4)$$

$$\Psi_M = -5 \left(\frac{z}{L}\right) \quad \text{for } L > 0 \quad (\text{if stable}) \quad (5)$$

With:

$$X = (1 - 16 \frac{z}{L})^{1/4} \quad L = \frac{\rho c_p u_* T_0}{kgH} \quad (6)$$

Assuming that the density of the air and the specific heat are constant, parameters to be determinate for the calculation of the Monin-Obukov length are the heat sensitive, the speed of friction and the roughness of the site where the pylon measurement is implanted.

2.1. Determination of Exchange by Sensible Heat

The sensible heat is defined as the amount of heat

exchanged without physical phase transition between several bodies forming an isolated system. It is described as "sensitive" because this heat exchange without the phase change modifies the body temperature, an effect that can be felt or measured by an observer. In this, the heat sensitive opposes the «latent heat», which is absorbed during a phase change, without changing the temperature. The sensible heat flux exchanged determined from an energy balance on the soil-air interface is used to write that the sum of the exchanged sensible heat flux H , latent heat E and convection G is equal to the net radiative exchange such that [14] :

$$H + E + G = Q \quad (7)$$

G : the exchanged flux by convection soil- air, W.m⁻².

H : the sensible heat flux soil-air, W.m⁻².

E : the flux exchanged solar latent heat, W.m⁻².

Q : the net exchange radiative soil-environment, W.m⁻².

The net flux exchanged by radiation between the surface and the environment is given by [9].

$$Q = (1 - r) * Ig - L^- \quad (8)$$

Where r is the albedo, L^- is the infrared radiation emitted by the ground and Ig is the overall incident illumination. After decomposition of the incident illumination to solar radiation emitted in the visible and in the infrared, it comes [13]:

$$Q = (1 - r) \left(\frac{I_{visible}}{Lg \text{ measure}}\right) Lg \text{ measure} + L^+ - L^- \quad (9)$$

$I_{visible}$: the solar irradiance emitted in the visible, W. m⁻²

Ig : the measured global solar irradiance W.m⁻²

L : the Monin - Obukov length, m.

L^+ : the incident infrared irradiance, W.m⁻²

L^- : Infrared emitted by the soil, W.m⁻²

Q : the net exchange radiative soil-environment, W.m⁻²

Assimilating the sun a black body , we can estimate that the ratio of visible light to the overall illumination is 0.588 .

$$Q = 0.588(1 - r)Ig \text{ measure} + L^+ - L^- \quad (10)$$

The incident infrared L^+ is a function of cloudiness Net that is estimated by [12] :

$$L^+ = C_1 T^6 + C_2 N \quad (11)$$

With N is equal to zero in clear sky and c_1, c_3, c_2 are proportionality coefficients that depend on the soil nature. Finally, assimilating the land to a black body, the infrared emitted by the soil is written as [12]:

$$L^- = \sigma T_s^4 \quad (12)$$

Whereas the equivalent soil temperature T_s is generally not measured, the previous expression is approximated by [13] :

$$L^- = \sigma T_0^4 + C_G Q \quad (13)$$

C_p : Specific heat of air at constant pressure $J. kg^{-1}K^{-1}$.

C_1 : Empirical constant [5] equal to $5.3.1. 10^{-12} W. m^{-2}.K^{-6}$.

C_2 : Constant empirically valid for altitudes equal to 60 $W.m^{-2}$ [5].

C_3, C_G : Coefficients depending on the nature of the soil.

Finally, the exchange of heat by convection is a function of net radiative flux Q as [12]:

$$G = C_G Q \tag{14}$$

Expression in which C_G represents the relationship between the heat flux emitted by the ground and the net radiative exchange [5]. Considering the fact that the measurement tower is located on a dry, on a dry and bare land, the flux of the latent heat E is zero (no water evaporation). Substituting in equation (10), the sensible heat is written [15]:

$$H = (1 - C_G) \frac{0.588(1-r)I_{g,mesuree} + C_1 T^6 - \sigma T^4 + C_2 N}{1 + C_3} \tag{15}$$

T_0 : the ambient temperature measured at 2m from the soil K.

T_s : the equivalent soil temperature K.

V : the wind speed $m.s^{-1}$.

K : the Von-Karman constant.

ρ : the air density, k/m^3

σ : the Stephan - Boltzmann Constant, $W.m^{-2}.K^{-4}$.

2.2. Atmospheric Boundary Layer (ABL)

The Atmospheric Boundary Layer (ABL) is defined as the part of the atmosphere where the presence of the Earth's surface (continental or oceanic) is directly sensitive. In fact, the whole atmosphere is influenced by the surface, but it is clear (by observation) that we can identify an area where the influence is "fast" [16]. This means that the atmosphere reacts with short time constants (of the order of the day maximum) to the surface stress. The rest of the atmosphere (the free troposphere, stratosphere and above) reacts with much longer time.

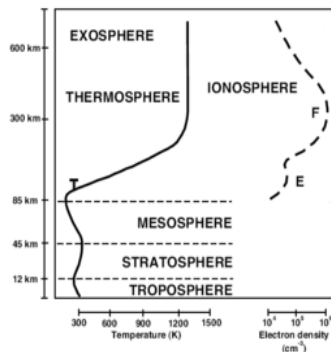


Figure 1. Atmospheric Boundary Layer (ABL).

2.3. The Albedo

The albedo is the ratio of solar energy reflected by a

surface to the incident solar energy. It is a dimensionless quantity, comparable to the reflectivity, but more specific application, it is used in astronomy and planetary science as well as geology. The word was introduced in the eighteenth century in optics and astronomy by the Swiss mathematician and astronomer Johann Heinrich Lambert. The albedo, in its most common definition called "Bond albedo" is a value between 0 and 1: a perfect black body, which absorbs all wave lengths without reflecting any, have a zero Albedo, while a perfect mirror, which reflect all wave lengths without absorbing one, have an Albedo equal to 1. Other definitions, including the geometric albedo can give values greater than 1.

Table 1. The albedo of different kind's surfaces.

Type of surface	Albedo (0 to 1)
Lake surface	0,02 to 0,04
Coniferous forest	0,05 to 0,15
Sea surface	0,05 to 0,15
dark soil	0,05 to 0,15
cultures	0,15 to 0,25
Light, dry sand	0,25 to 0,45
Limestone	environ 0,40
ice	environ 0,60
packed snow	0,40 to 0,70
fresh snow	0,75 to 0,90
perfect mirror	1

The Earth-atmosphere system is the fraction of solar energy reflected back into space. Its value lies between 0 and 1. More reflective a surface is, the higher is its Albedo. The elements that contribute most to the Albedo of the Earth are: clouds, snow and ice surfaces, aerosols. For example, the albedo of fresh snow is 0.87, meaning that 87% of solar energy is reflected by this type of snow.

3. Results and Discussion

3.1. Mast Measurement

3.1.1. Wind Farm Koudia Al- Baida

The Wind Park Koudia Al Baida is situated on the site of the same name, between the cities of Tangier and Tetouan. With an installed capacity of 54 MW. Operational since 2000, the park Al Baida Koudia, is the largest facility of its kind in Africa.



Figure 2. Wind farm Koudia Al- baida.

The pylon of measures of meteorological parameters was implemented by the Centre for the Development of Renewable Energy (CDER) at the weather station of watershed Al Koudia al Baida (the region Tanger-Tetouan). Located in the Moroccan highlands, the latter is considered a semi-arid area with a dry and harsh climate, very hot in summer and often very cold in winter. Each of the 5 levels and masts 2 and 4m, have a ENERCO station comprising an acquisition unit and sensor measurements. Measurements of temperature, of the overall illumination and of the wind speed are taken every 10 m.

Table 2. Proportion of bioclimatic zones in the region of Al Baida Koudia al - Tetouan Ksar Sghir [18].

Variant	cold	fresh	doux	temperate	total area (%)
Sub humid	0.4	-	-	-	0.4
Semi arid	17.8	2.9	-	-	20.7
Arid	6.4	18.2	1.7	-	26.3
Per arid	0.8	11.2	17.8	22.7	52.6
Total area (%)	25.4	32.3	19.5	22.7	100

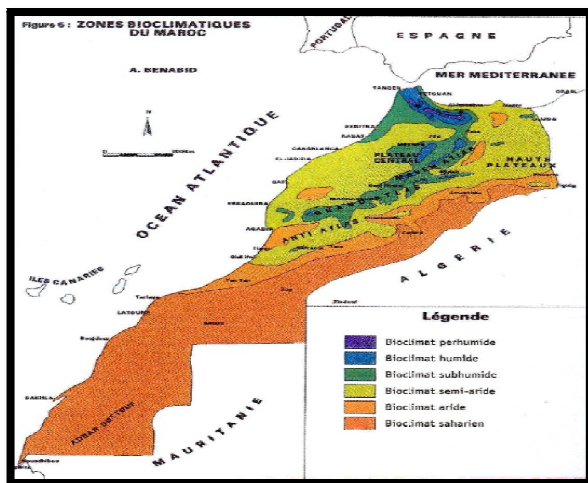


Figure 3. Bioclimatic zones of Morocco.

Figure 3 shows the distribution of 10 different bioclimatic units within the basin Al Koudia al Baida. The per arid bioclimate in its thermal variations temperate and cool includes broader regions (approximately 40%, Table 2). These regions generally correspond to vegetation units dominated by Saharan flora. The perarid bioclimates cold, arid cold and arid very cold dominates the mountain. In total, this class of bioclimate covers about 35% of the Tanger- Tetouan region. These areas are mainly characterized by sagebrush steppes of Ibero- Mauritanian and are the main routes for transhumance pastoralist's autumn to spring. The semi-arid bioclimatic in the cold to very cold variant characterize 20% of the region [15]. It is limited to high mountain ranges along the line of the watershed northwest of the basin Al Koudia Al Baida. In these areas, the vegetation changes to a thorny xerophytic

used especially in summer for pasture to sheep and goats.

3.2. Exchange by Sensible Heat

Since the implantation site of the pylon is semi-arid, the coefficients C_G and C_3 are taken equal to 0.1 and 0.38 respectively [5]. The average cloud cover and albedo (dry sand) are estimated respectively to 0.3 and 0.25 [8]. A numerical simulation based on an iterative method was developed for the calculation of the exchange by sensible heat. In Figure 1 are plotted the overall incident illumination I_g and the amount of sensible heat H , according to atmospheric stability classes. The latter varies between -50 and 290 W/m^2 . Knowing that for positive values of H , atmospheric conditions are unstable (air masses heat up and rise), for negative H conditions are stable (air masses cool and down) and for near-zero conditions are neutral, various measures have been classified. The results show that the transition from stable to unstable conditions happens when the solar irradiance reaches 14 % of maximum.

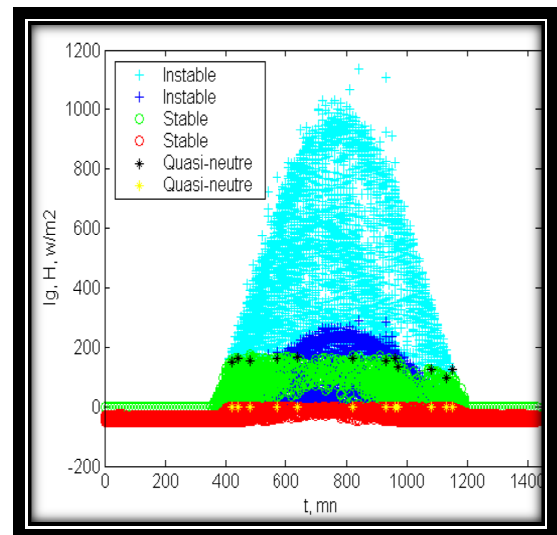


Figure 4. Changes in global illumination and sensible heat flux exchanged according to the -class of stability [19, 20].

3.3. Calculation of the Roughness and the Friction Velocity

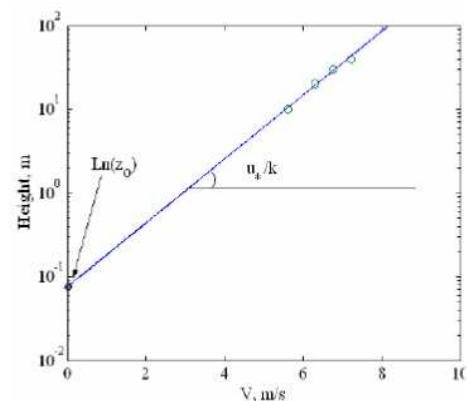


Figure 5. Determination of the surface roughness and the friction velocity.

In Figure 5 is shown the linear fitting curve of wind speed versus $\log(z)$. The intersection with the y axis allows the determination of the soil roughness which is estimated at 0.0847 m. Value quite similar to that provided by the National Office of Meteorology for the concerned site (0.09m). Moreover, the friction velocity representative tangent is equal to 0.4556

3.4. Vertical Velocity Profile

The determination of the flux of sensible heat, the friction velocity and the soil roughness allows the computation of the Monin Obukov length [1] using equation 6 and the separation of the data according to the class of stability. On 16986 data representing the measurement period, 75 % is stable class and 25 % unstable class. In Figure 6 are plotted the vertical profiles of wind speed according to the class of stability and globally regardless of the class. For unstable conditions, the movement of air is strongly turbulent. These conditions occur during the day and especially during sunrise. The friction is then small in relation to the turbulence ($U_* = 0.2975$). Finally, profiles of the wind speed, in stable conditions and regardless of the class have the same pattern and tend to join with altitude. These conditions usually occur during the night or in cloudy sky. Friction on the soil is then higher.

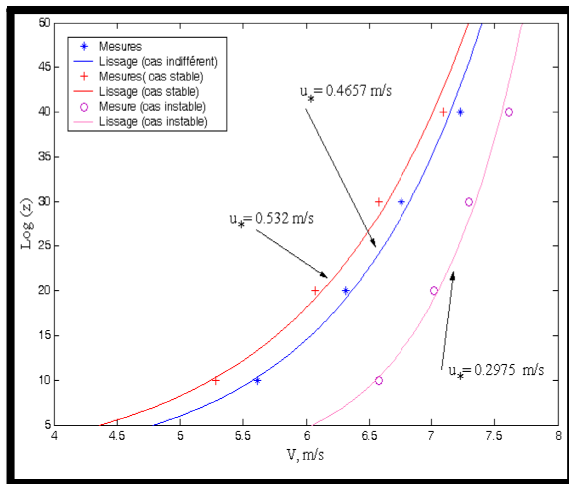


Figure 6. logarithmic profile of the wind speed according and regardless of the class of stability.

4. Conclusion

In the present work, we presented a method that allows the characterization of the vertical wind profile in the atmospheric boundary layer. This is obtained from the measurement of solar irradiance incident, ambient temperature and wind speed at different levels. This allowed the characterization of the profile of the wind speed for a semi- arid zone. Indeed, the weather conditions are very sensitive to climate. The transition from stable to unstable class of stability occurs when the solar irradiance is 14 % of its maximum reached. The results show that the

vertical profile of the wind speed varies according to the class of atmospheric stability (stable or unstable). Furthermore, the neutrality hypothesis raised by several authors is unfounded. Finally, it should be noted that the neutral stability conditions are very difficult to identify (H close to zero), only 10 measures on 16986 were identified.

References

- [1] Dr. Gary & L. Johnson, «Wind Energy Systems», Available: 2007www.rpc.com.au/ products/wind turbines/wind book/WindTOC.html
- [2] J.F. Man well, J.G. McGowan & A.L. Rogers, «wind energy explained», John Wiley & Sons Ltd: 2008.
- [3] J.P. Norton, “an introduction to identification”.Academic press, 1986.
- [4] Régis Bourbonnais, « Analyse des séries temporelles », Dunod - 2e édition ,336 pages – 2008
- [5] C.GourierouxA. Montfort, « Série temporelles et modèles dynamiques », 664 pages 2010.
- [6] GUGLIELMI Michel, « Signaux aléatoires : modélisation, estimation, détection (Traité IC2, série traitement du signal et de l'image) », Lavoisier ,374p, 2011
- [7] "Le spectaculaire développement de l'énergie éolienne en Espagne »Congress EWEC 2010 Available:www.clean-auto.com. /spip.php?article 1334
- [8] J.F. Manwell, J.G. McGowan & A.L. Rogers, «wind energy explained», John Wiley & Sons Ltd: 2010, ch 2.
- [9] William David Lubitz, "Accuracy of Vertically Extrapolating Meteorological Tower Wind Speed Measurements", Canadian Wind
- [10] A.S. Monin ET A.M. Obukov, Basic Regularity in Turbulent Mixing Surfaces Layer of the Atmospheric. Akad. Nauk. S.S.S.R...TrusdGeof. Inst., Volume 24, pp 151, 1954.
- [11] A.J. Dyer, A Review of Flux Profile Relationships, Int. J. Boundary Layer Meteorology, Volume 7, pp, 363-372, 1974.
- [12] C.A. Paulson, The Mathematical Representation of Wind Speed and Temperature Profiles in the Unstable Atmospheric Surface Layer, Int. J. Applied Meteorology, 1970.
- [13] B. Itier, Une Méthode Simplifiée pour la Mesure du Flux de Chaleur Sensible, J. Recherché Atmosphérique Volume 14/1, pp17-44, 1980.
- [14] A.A.M. Holtslaget A.P. Van Ulden, A Simple Scheme for Daytime Estimates of the Surface Fluxes from Routine Weather Data, J. Climate Ap. Meteorology, Vol. 22/4, 1983.
- [15] N. bassiralhssen, Evaluation du Gisement Energétique Eolien. Contribution à la Détermination du Profil Vertical de la Vitesse du Vent en Algérie. Thèse de doctorat D'état en physique énergétique, Université de Tlemcen, 2010.
- [16] A.Benaboud, M.Hajjoubi, M.Ahd, A.Erkik, A.Echchel Evaluation And Statistical Analysis Of Potential Wind The Wilaya Tanger-Tetouan TSIIJ Env. Sci.Vol 8, Vol.8Issues 6, pp: 1-19, 2013.

- [17] M. Mrabet, Contribution à la Détermination des Performances Théoriques et Expérimentales des Capteurs Solaires à Tubes Sous-virent en Régime Transitoire. Thèse de Doctorat d'état en physique énergétique, Université de Tlemcen, 2011.
- [18] M. Capderou, Atlas Solaire de l'Algérie. Modèles Théoriques et Expérimentaux. Office Des Publications Universitaire, mai 2010.
- [19] KARROUK. M.S (2003) : Dynamique des climat du Maroc ; thèse de doctorat d'état ; université Hassan II faculté des Lettres et des Sciences humaines Ben M'sik. Casablanca.
- [20] KARROUK. M.S (1987): Le climat de la péninsule tingitane; thèse de doctorat de 3ème cycle; université de paris Sorbonne dpt de géographie physique 09, institut de géographie. Paris